Biosensors and Bioelectronics 68 (2015) 34–40

Contents lists available at ScienceDirect

Biosensors and Bioelectronics

journal homepage: www.elsevier.com/locate/bios

A whole-cell electrochemical biosensing system based on bacterial inward electron flow for fumarate quantification

Rong-Wei Si [a,1], Dan-Dan Zhai [a,b,1], Zhi-Hong Liao [a], Lu Gao [a], Yang-Chun Yong [a,*]

[a] Biofuels Institute, School of the Environment, Jiangsu University, 301 Xuefu Road, Zhenjiang 212013, Jiangsu Province, China
[b] College of Biological Engineering, Henan University of Technology, Zhengzhou 450001, Henan Province, China

ARTICLE INFO

Article history:
Received 24 September 2014
Received in revised form
8 December 2014
Accepted 15 December 2014
Available online 16 December 2014

Keywords:
Oncometabolite
Fumarate
Biosensor
Microbial fuel cells
Bioelectrochemical system

ABSTRACT

Fumarate is of great importance as it is an oncometabolite as well as food spoilage indicator. However, cost-effective and fast quantification method for fumarate is lacking although it is urgently required. This work developed an electrochemical whole-cell biosensing system for fumarate quantification. A sensitive inwards electric output (electron flow from electrode into bacteria) responded to fumarate in *Shewanella oneidensis* MR-1 was characterized, and an electrochemical fumarate biosensing system was developed without genetic engineering. The biosensing system delivered symmetric current peak immediately upon fumarate addition, where the peak area increased in proportion to the increasing fumarate concentration with a wide range of 2 μM–10 mM (R^2=0.9997). The limit of detection (LOD) and the limit of quantification (LOQ) are 0.83 μM and 1.2 μM, respectively. This biosensing system displayed remarkable specificity to fumarate against other possible interferences. It was also successfully applied to samples of apple juice and kidney tissue. This study added new dimension to electrochemical biosensor design, and provide a simple, cost-effective, fast and robust tool for fumarate quantification.

1. Introduction

Fumarate is a key intermediate in the tricarboxylic acid cycle (Kerbs cycle) and plays crucial roles in the fundamental processes of energy metabolism as well as lipids and amino acids biosynthesis. Abnormal accumulation of fumarate due to fumarate hydratase (FH, responsible for hydration of fumarate to malate, also served as tumor suppressor) mutation is one of the main causes of hereditary leiomyomatosis and renal cell cancer (the top 10 most common malignancies) (King et al., 2006; Pollard et al., 2005; Siegel et al., 2012; Tomlinson et al., 2002; Toro et al., 2003). Therefore, it is considered to be an oncometabolite (Yang et al., 2012, 2013), and might be a potential biomarker for early diagnosis of FH-associated cancer diseases. Besides, fumarate also presented in beverages, baking powders and candy due to microbial spoilage or impurity from synthetic additives (Kvasnicka and Voldrich, 2000; Lee and Wrolstad, 1988), and thus becomes an important indicator for quality inspection of food products (Kvasnicka and Voldrich, 2000; Trifiro et al., 1997).

So, development of new methods for fast, sensitive, and cost-effective detection of fumarate are of great interest and importance for disease diagnosis, cancer research and food quality control/inspection. High-performance liquid chromatography (HPLC) and ion chromatography are commonly used for fumarate determination in different fruit juices or animal samples (Baati et al., 2011; Jham et al., 2002; Kvasnicka and Voldrich, 2000; Trifiro et al., 1997). After methyl- or butyl-esters derivation, gas chromatography (GC) analysis was applied for fumarate detection in different food samples (Barden et al., 1997; Jham et al., 2002). Capillary isotachophoresis (cITP) combined with capillary zone electrophoresis, or capillary electrophoresis-mass spectrometry were developed for sensitive quantification of fumarate in fruit juice, feed additive, or plant leaves (Blatny et al., 1996; Kvasnicka and Voldrich, 2000; Wakayama et al., 2010). But the problems associated with these physic-chemical methods include complicated sample pretreatment (solid phase extraction or derivation), or expensive equipment, or low specificity (Table S1).

Biosensing provides an alternative analytical method with low cost, high specificity and high sensitivity (Su et al., 2011; Yong and Zhong, 2009). More impressively, whole-cell biosensor is able to provide unique bioavailability information of analytes which other methods are incapable of (Su et al., 2011). Up to date, there is only one whole-cell biosensor for fumarate detection was developed (Ganesh et al., 2013). By fusing a GFP protein with a well-designed chmimeric DcuS/EnvZ two component system, Ganesh et al. (Ganesh et al., 2013) developed a fumarate biosensor by using *Escherichia coli* cells. This biosensor produced GFP fluorescence in

* Corresponding author. Fax: +86 511 8879 0955.
E-mail address: ycyong@ujs.edu.cn (Y.-C. Yong).
[1] Equal contribution.

http://dx.doi.org/10.1016/j.bios.2014.12.035
0956-5663/

response to fumarate and was used for fumarate quantification with the help of a fluorospectrophotometer (Table S1). However, this traditional whole-cell biosensor need complicated strain modification process with genetic engineering, and can not provide readable output (electric signaling) without complicated equipment, which in turn limited its application.

Electrochemical whole-cell biosensor, which directly delivered readable electric output without additional transducer, was considered as one of the most promising biosensing method (Golitsch et al., 2013; Wang et al., 2013; Webster et al., 2014). Thus, this work, for the first time, attempted to develop an electrochemical whole-cell biosensor for fumarate quantification. In *Shewanella oneidensis* MR-1 cells, the electrons from solid electrode could be passed to cells (bacterial inwards electron transfer) (Li et al., 2014; Ross et al., 2011; Thomas et al., 2013; Wu et al., 2013; Yong et al., 2014). As fumarate reductatse directly linked with bacterial outer-membrane redox proteins responsible for electron transfer (Li et al., 2014; Ross et al., 2011), we proposed that, the inward electrons would be used for fumarate reduction, and thus the change of inwards current might serve as output signal to reflect the fluctuation of exogenously added fumarate (input) (Fig. 1a). In the light of the unique character of *S. oneidensis* MR-1, an electrochemical whole-cell biosensor for fast, sensitive, and selective quantification of fumarate was developed, and was successfully applied to analyze the food and tissue samples.

2. Materials and methods

2.1. Bacteria culture

LB broth (peptone 10 g/L, yeast extract 5 g/L, NaCl 5 g/L, pH 7.0) was used as the growth medium for *S. oneidensis* MR-1 in suspension culture. Glycerol stocks of *S. oneidensis* MR-1 was streaked on LB agar plate and grown overnight at 30 °C. A single colony was inoculated to 5 ml fresh LB medium and cultivated overnight at 30 °C with shaking (200 rpm). Then, 0.5% (v/v) inoculum was pipetted into LB medium and cultivated at 30 °C with shaking (200 rpm), cells were harvested by centrifugation, then re-suspended in the anolyte (5% LB medium and 95% M9 minimal medium, 18 mM lactate) (Peng et al., 2010; Yong et al., 2014; Yu et al., 2011). The cell suspensions were transferred into the three-electrode electrochemical cell (120 mL or 12 mL) and the test was performed at room temperature.

2.2. Sample preparation

All animal experimental procedures have been reviewed and approved by the Animal Experimentation Ethics Committee of the Faculty of Pharmacy of Jiangsu University, China. The study has been performed using female Wistar rats. Kidney samples were prepared as described elsewhere with minor modification (Baati et al., 2011). Kidney were extracted, washed with a 0.9% NaCl solution and stored at −20 °C until analysis. 0.5 g of kidneys was added to 0.5 mL of SDS (0.1 M) in 10 mL glass tubes, and spiked with different amount of fumarate. After homogenization, 1 mL of phosphate buffer (0.04 M, pH=2.5), 1.5 mL of methanol and 1 mL of acetonitrile were added. Then, the mixture was stirred for 1 h at room temperature. After centrifugation (8000 × *g*, 10 min), the organic phase was collected and filtered through a 0.22 μm sterile syringe filter. The pellet was extracted again under the same conditions. Then, the supernatant of extraction was pooled and evaporated at 40 °C, and the dry residue was dissolved in 0.5 mL Mili-Q water for further biosensing assay.

For apple juice samples, 5 mL fresh apple juice (spiked with different amount of fumarate) or spoiled apple juice (mold

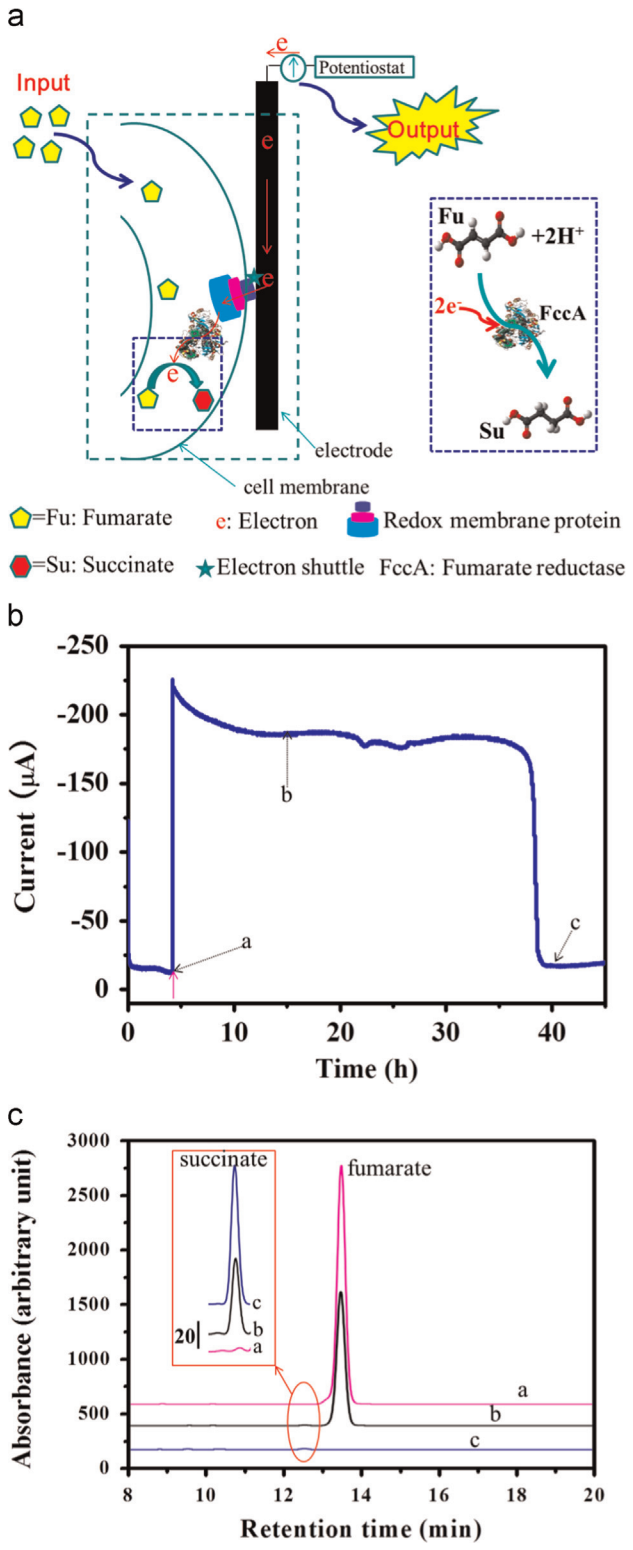

Fig. 1. (a) Schematic of the developed biosensing system (Inset is the mechanism of fumarate transformation catalyzed by fumarate reductase). (b) The electric response of *S. oneidensis* MR-1 to fuamrate (the pink solid arrow indicates the injection of the fumarate, the dotted line arrows indicates sampling points for HPLC analysis in Fig. 1c). (c) HPLC analysis of fumarate and succinate transformation during the bioelectrochemical catalysis process (Inset is the enlarged view of the selected area; pink line (line a) indicates the HPLC profile of the sample immediately taken after fumarate addition (point 'a' shown in Fig. 1b); black line (line b) represents the sample taken at the mid-phase of the bioelectrochemical reaction (point 'b' shown in Fig. 1b); blue line (line c) represents the sample taken at the end of the bioelectrochemical reaction (point 'c' shown in Fig. 1b)).

contaminated apple juice incubated at 30 °C for different days) was extracted with 10 mL ethyl acetate for three times. Then, the organic phase was pooled, filtrated and evaporated to dryness at 40 °C. The residue was dissolved in 0.5 mL Mili-Q water for further biosensing assay.

2.3. HPLC analysis

The concentrations of fumarate and succinate were quantitatively analyzed by HPLC (Shimadzu, Japan) equipped with a C18 column (5 μm particle size, 250 mm × 4.6 mm i.d.) (Baati et al., 2011; Ryu et al., 1999). The mobile phase consists of acetonitrile, water and phosphoric acid in the ratio of 2:98:0.05 (v/v/v), and the flow rate used is 0.5 mL/min. The column temperature is 35 °C and the wavelength of detection is 210 nm.

2.4. Bioelectrochemical system (BES) setup

All electrochemical measurements were carried out with CHI 660E electrochemical workstation or CHI1000B potentiostat (Chenhua Instruments Co., Ltd., Shanghai, China). A platinum wire electrode and a saturated calomel electrode (SCE) were used as counter electrode and reference electrode, respectively. A 4 cm × 4 cm or 1 cm × 1.6 cm carbon cloth pretreated with acetone and HCl was used as the working electrode. The BES operation was conducted in a 120 mL or 12 mL glass bottle with three electrodes inserted through the cap. All potentials are reported *vs.* SCE.

2.5. Biosensing assay

Biosensing assay was conducted in three-electrode BES cell. When bacterial suspension (suspended in electrolyte) was transferred into a sterile BES cell, the potential of the working electrode was poised at −0.6 V (*vs.* SCE) using CHI1000B potentiostat. After about 30 min of acclimation under the poised, different volume of concentrated fumarate solution (1 M) or fumarate samples was added into each BES cell. The BES cell without fumarate addition served as the control. The change of the current upon fumarate addition was continuously monitored by a potentiostat (CHI1000B, Chenhua Instrument Co., Ltd., Shanghai, China).

3. Results and discussion

3.1. Biosensing system development

In order to develop the electrochemical biosensing system, a sensing module/protein, which specifically responded to the analyte and had electrochemical activity, should be screened out first. Fumarate reductase, which specifically catalyzed a fumarate reduction accompanied by electron transfer (Leys et al., 1999; Ross et al., 2011), was considered to be a potential candidate. Interestingly, *S. oneidensis* MR-1 contained a unique fumarate reductase localized to the periplasmic and actively interacted with the cell membrane associated electron transfer pathway (Li et al., 2014; Ross et al., 2011) (Fig. 1a). The fumarate reduction was investigated by using cyclic voltammetry. In accordance with previous report (Ross et al., 2011), upon addition of fumarate, a catalytic waveform with a mid-point potential of ~0.6 V (*vs.* SCE) corresponding to fumarate reduction was observed (Fig. S1). Thus, based on the cyclic voltammetry result (Fig. S1) and previous reports (Ross et al., 2011; Yong et al., 2014), the potential of −0.6 V was used to enable the fumarate reduction. Next, the relationship between electron transfer and fumarate reduction of *S. oneidensis* MR-1 was further investigated in a BES cell with three-electrode system. When the anode was poised at −0.6 V, a negative current

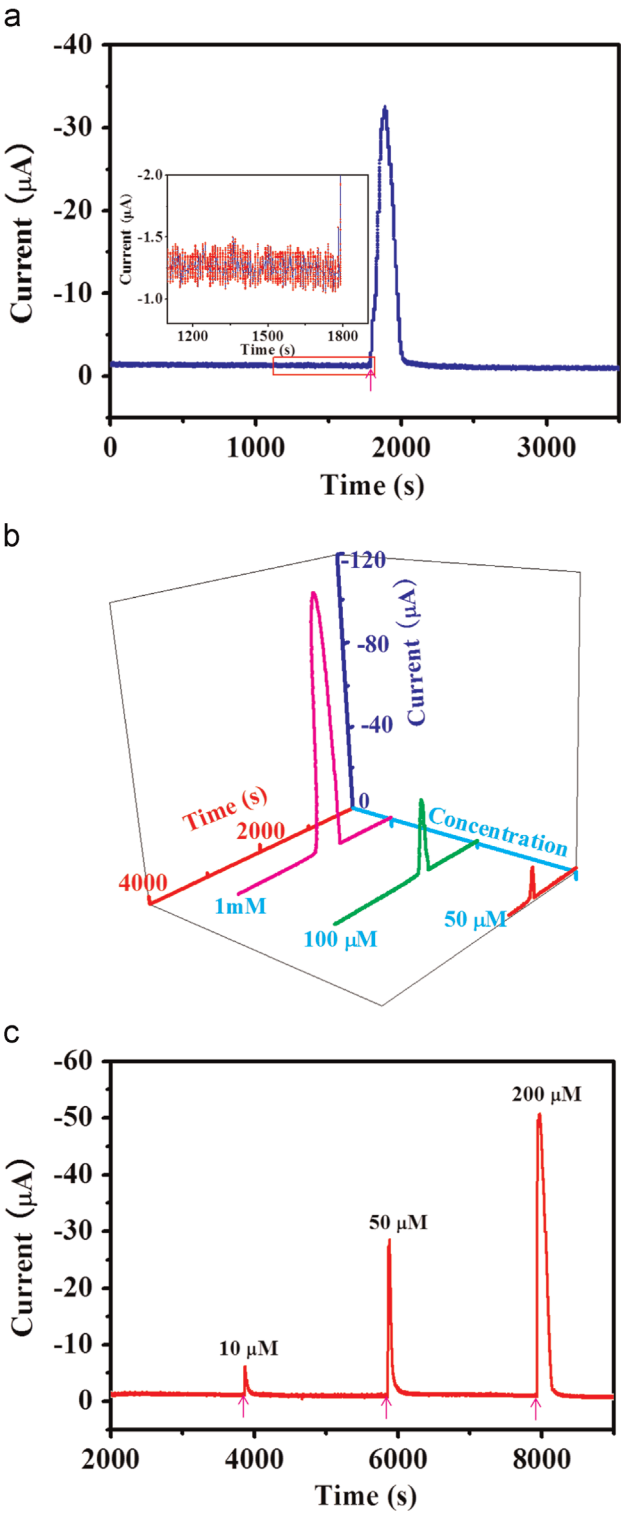

Fig. 2. Biosensor dose-dependent response to fumarate. (a) Current baseline and biosensor response to 100 μM furmarate (Inset is the enlarged view of the selected area for baseline assessment). (b) Biosensor response to fumarate with different concentration (batch mode, 50 μM, 100 μM, and 1 mM). (c) Biosensor response to successively added fumarate. The arrow indicates the injection of the fumarate.

represents inward electron transfer (defined as electrons flow from the electrode into cells) increased immediately upon fumarate addition, while it decreased to the baseline level once the fumarate was exhausted (Fig. 1b and c). However, this inward

current could be abolished by disruption of fumarate reductase or electron transfer related membrane proteins (Ross et al., 2011). More interestingly, fumarate consumption and succinate production during inward electron transfer process which corresponding to fumarate reduction was observed as determined by HPLC analysis (Fig. 1c). These results implied that the inward current linked to fumarate reduction in *S. oneidensis* MR-1. Thus, it is likely to use this inward electron flow for fumarate (Fig. 1a).

Then, the analytical reliability of this *S. oneidensis* MR-1 BES cell was tested. As expected, a stable current (attributed to the reduction of redox enzymes and electron shuttles in the *S. oneidensis* cells and the electrolyte) with little fluctuation (1.26 ± 0.09 μA) which could be served as baseline was obtained only several minutes after the poised potential (-0.6 V) was applied on the anode of BES cell (Fig. 2a). Compared with other mediator-less whole-cell bioelectrochemical biosensors (Kim et al., 2003; Wang et al., 2013) in which a biofilm development process is indispensable to get stable baseline, the time for stabilization in the assay developed here is much shorter as there is no need of biofilm formation process. More strikingly, upon fumarate (100 μM) injection, the current output immediately increased and reached the peak current within about 110 s (Fig. 2a). Further, the current output signal decreased quickly to the baseline, which resulted in a uniform current peak in response to fumarate addition (Fig. 2a). Thus, this biosensing system consists of a three-electrode BES cell with *S. oneidensis* MR-1 suspension could be used for fumarate detection, and it is likely to develop a quantification method for fumarate by using the current peak as the biosensing output.

The amount of the catalyst used largely affected the biosensing output and should be optimized. For whole-cell system, it was usually determined by the specific enzyme activity and cell amount (or cell concentration with a fixed volume). In this study, the specific enzyme activity of fumarate reductase showed good correlation with the cell growth phase, and reached its highest activity at the early stationary growth phase (16 h) (Fig. S2a and b). Moreover, optimization based on the intensity of biosensor output was performed and the result indicated 16 h was the optimum cultivation time (Fig. S2c), which was in good agreement with the results of enzyme activity. Thus, cultivation time of 16 h under strict cultivation conditions (inoculum size 0.5% (v/v), LB medium, 30 °C, 200 rpm) were fixed to get the optimum biosensor output. The consistence of specific enzyme activity of cells (i.e., fumarate reductase activity per cell in this study) could be guaranteed by strictly controlling the cultivation time in well-defined culture conditions as previous reports (Schenkmayerova et al., 2013; Tang et al., 2014). Because the microbial enzyme expression usually correlated with the cell growth, and the cell growth profile was well reproducible under the same culture conditions. Then, the cell concentration used was optimized based on the peak current upon fumarate addition, and an optimized concentration of $OD_{600}=1.5$ ($1.5 \pm 0.1 \times 10^8$ CFU/mL) was selected for further experiment (Fig. S2d).

3.2. Quantification of fumarate with the developed biosensing system

Next, the concentration response to fumarate by the developed biosensing system was determined in order to achieve quantitative assay. Upon the addition of different concentrations of fumarate, the current output immediately increased and formed uniform peaks with different height and area, respectively (Fig. 2b). As the current output quickly decreased to baseline level once the fumarate reduction completed and fumarate was exhausted (Figs. 1 and 2), it is possible to successively detect the fumarate by using this biosensing system. As shown in Fig. 2c, when different concentration of fumarate was successively added into the biosensing system, uniform and separate current peak series were obtained, which suggested that the developed system could be used for on-line/continuous monitoring.

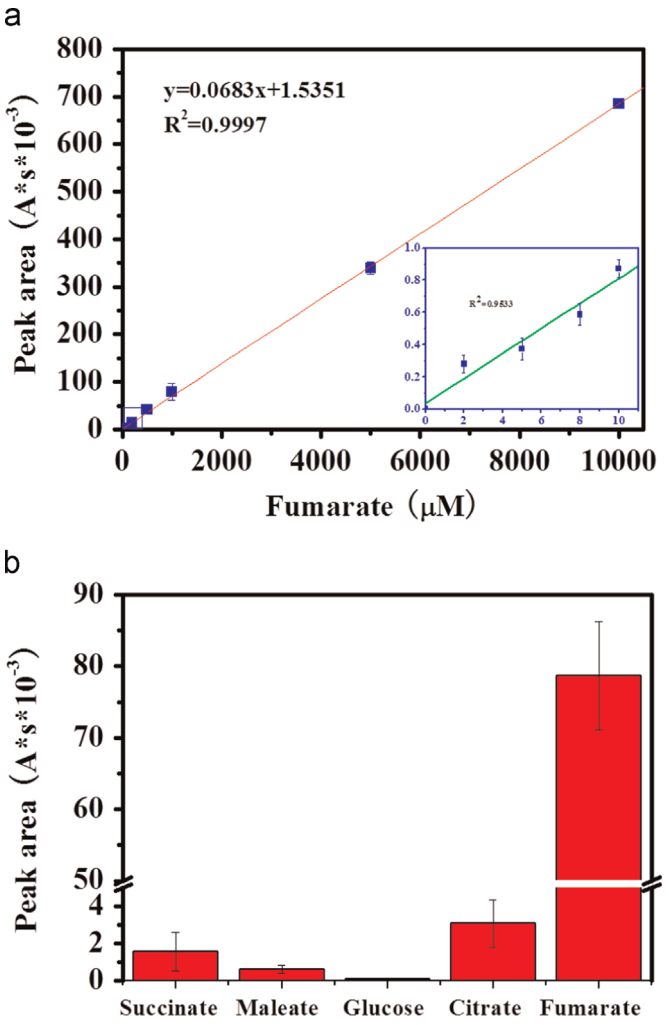

Fig. 3. (a) Linear calibration curve based on the relationship between output current peak area and fumarate concentration (Inset is the enlarged view of the selected low concentration area). (b) Effect of interferences (1 mM) on biosensor response.

The calibration curve of this biosensing system was then determined. As the current output represents the inward electrons that were consumed by the fumarate reduction, the charge (corresponding to total electrons) transferred from the electrode to the cells should reflect the fumarate amount added (as well as the concentration in fixed volume). Therefore, the current peak area corresponding to total charge transferred might be in proportional to the fumarate amount/concentration. The relationship between fumarate concentration and current peak area were analyzed. As indicated in Fig. 3a, the peak area showed good linear relationship ($R^2=0.9997$) with the fumarate concentration ranging from 2 μM to 10 mM. The limit of detection (LOD, defined as 3 times of baseline noise (Yong and Zhong, 2009)) determined was 0.83 μM ($S/N=3$), while the limit of quantification (LOQ, defined as 10 times of baseline noise (Yong and Zhong, 2009)) determined was 1.2 μM ($S/N=10$). Compared with the conventional physic-chemical methods, the LOD obtained by this system is about 20 times lower than chemometric method (Sokullu et al., 2010) and about 2 times lower than HPLC method (Baati et al., 2011), and also with a much wider detection range. More impressively, the system developed here showed about 2 orders of magnitude lower LOD

than the reported sole fumarate whole-cell biosensor (Ganesh et al., 2013).

Specificity is one of the most important parameters for an analytical method. Thus, different possible interferences with similar molecular structure to fumarate (succinate, citrate and maleate) and the most predominant organic compound (glucose) were added into the biosensing system, the electric output was monitored respectively. As shown in Fig. 3b, for all of these possible interferences analyzed, the relative response delivered is negligible ($<4\%$). For example, glucose and maleate only delivered less than 1% relative response compared to fumarate. For succinate, the product of fumarate reduction, only marginal relative response (1.9%) was observed. The results indicated the biosensing system developed here was highly specific to fumarate which might ascribe to the substrate specificity of fumarate reductase.

Moreover, possible interference from microbe contamination during sample injection is another concern for practical application. As the electrochemical interaction between the fumarate reductase and outer-membrane redox proteins (the key mechanism for electrochemical response to fumrate) is unique to *S. oneidensis* (Ross et al., 2011), other bacteria such as *E. coli* and *Pseudomonas aeruginosa* did not produce significant response to fumarate addition under the biosensing conditions used here. In addition, microbial contamination from sample injection also did not significantly affect the biosensor output (Fig. S3). These results suggested that this biosensing system was robust enough and was promising for further practical applications. However, microbial contamination should be always taken into account (esp. for long-term operation), further work on special device design, genetic engineering, or cell immobilization might be useful to eliminate the possible effect of microbial contamination.

The storage stability was evaluated by measuring the response of this closed biosensing system stored at 4 °C during the testing period. It was found that this biosensing system had good storage stability for at least 10 days (Fig. 4a). The good long-term storage stability might ascribe to the excellent low temperature resistance of *S. oneidensis* MR-1 (Abboud et al., 2005). Furthermore, the reusability was investigated with 100 μM fumarate. Impressively, about 94–101% relative biosensor output was obtained during 30 times successive detection (Fig. 4b), which suggested that this biosensing system could be reused for at least 30 times.

3.3. Application to different samples

To establish the credibility of this newly developed biosensing method, various samples contained different amount of fumarate were tested. As shown in Table 1, the fumarate amount in the water samples quantified by the biosensing system was in good agreement with the real amount spiked. The recovery of all measured samples was between 92% and 120%, while the coefficient of variation (CV) was between 1.7% and 11%. The results indicated this biosensing system is reliable towards fumarate quantification.

As fumarate quantification is of great importance for food industry and disease diagnosis, apple juice or mice kidney spiked with different amount of fumarate served as the synthetic spoiled food or tumor samples were analyzed using the developed biosensing system. There was no significant detectable biosensor output was obtained when applied to the fresh apple juice and mice kidney samples without fumarate addition (control samples), which indicated the possible interference from food and tissue samples was negligible. When the synthetic spoiled food or tumor samples (the fumarate concentration used here covered the reported representative fumarate concentration in real samples (Pollard et al., 2005)) were applied, the fumarate concentration was quantified by the developed biosensing system and HPLC,

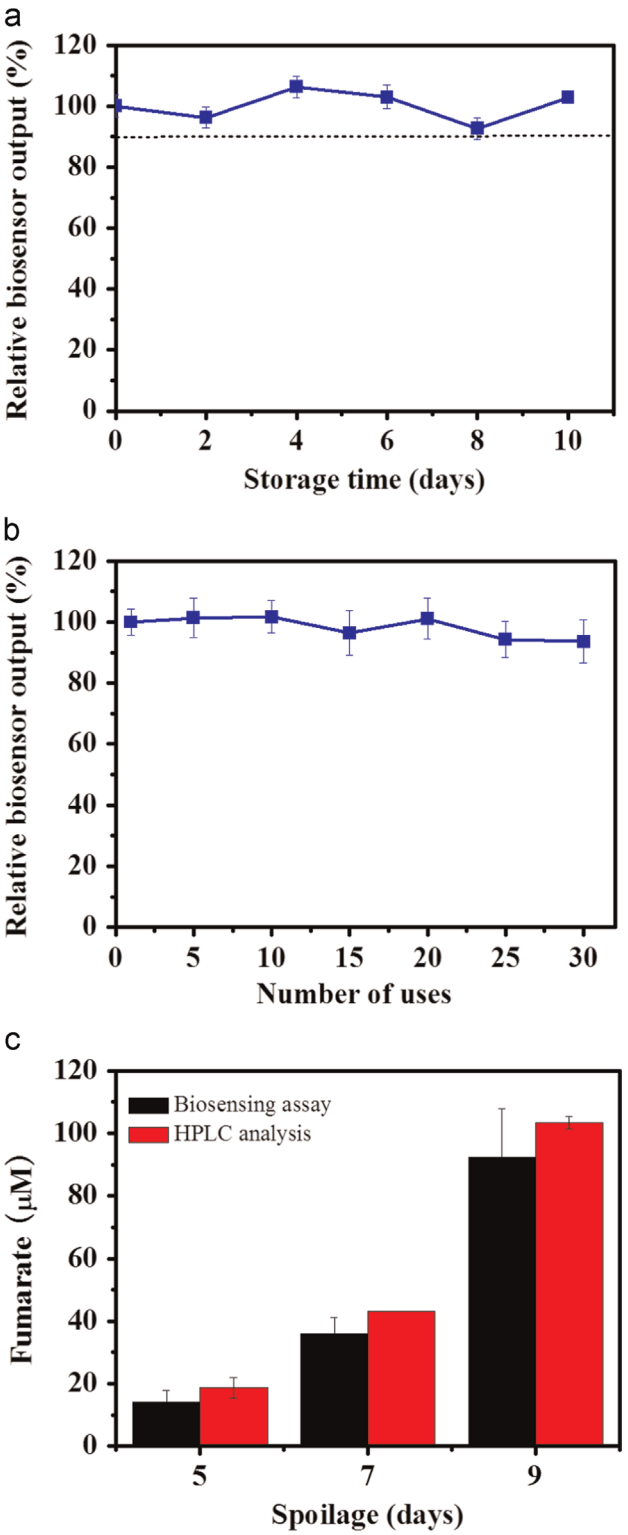

Fig. 4. (a) Long-term storage stability and (b) reusability of this whole-cell biosensing system. (c) Fumarate quantification for spoiled apple juice contaminated by mold with biosensing assay and HPLC analysis, respectively. *X*-axis indicates the time for samples incubation with spoilage mold before analysis. Statistical significance of differences was analyzed by *t*-test (biosensing assay *vs.* HPLC assay for the same sample), and no significant difference ($P>0.1$) was observed between the results from biosensing assay and HPLC assay.

respectively. As shown in Table 2, the quantification results obtained corresponded well to their real concentration as well as the HPLC quantification results with high recovery (91.2–113%) and low CV (3.1–8.2%). Furthermore, apple juice spoiled by mold was

Table 1
Quantification results of water samples spiked with authentic fumarate.

Fumarate (μM)		CV[a](%)	Recovery (%)
Spiked	Determined by biosensor (mean)		
4.00	4.03	6.4	101
31.0	29.4	3.4	94.9
100	92.5	11	92.5
600	630	7.6	105
2000	2400	1.7	120
7000	6917	4.8	98.8

[a] CV, coefficient of variation ($n=3$).

Table 2
Quantification results of synthetic food or tissue samples.

Fumarate			CV[a](%)	Recovery[b] (%)
Addition	Determined by			
	HPLC (mean)	biosensor (mean)		
Apple juice (μM)				
10	10.3	10.4	3.1	104
50	49.6	45.6	5.2	91.2
250	289	282	6.9	113
Mice Kidney (mg g^{-1}/μM)				
0.30/80	NT[c]	0.30/80	8.2	100
0.58/150	NT	0.56/145	5.5	96.6
1.34/350	NT	1.25/327	5.5	93.3

[a] CV, coefficient of variation ($n=3$) for biosensor assay.
[b] Recovery for biosensor assay.
[c] Not tested.

analyzed by the developed biosensing assay and HPLC, respectively. The fumarate concentration quantified by the biosensing assay was in accordance with the HPLC analysis, which showed a significant increase on fumarate concentration with the prolonged incubation/spoilage time (Fig. 4c). Interestingly, the fumarate concentration from biosensing assay was a little lower (although not significant) than that from HPLC assay (Fig. 4c), which might due to the biosensing assay was only accessible to the bioavailable fraction while the HPLC assay detected the total amount without bioavailability information (D'Souza 2001). This is one of the advantages of the biosensing assay (bioavailability information) over the physic-chemical assay (D'Souza 2001). The results verified that fumarate would be served as an indicator for food spoilage and confirmed that this biosensing assay had good reliability and validity for different samples.

4. Conclusion

An electrochemical biosensing system based on bacterial inward electron transfer was developed by using *S. oneidensis* MR-1. When the working electrode was posied at −0.6 V, a stable baseline was obtained within 10 min with little fluctuation. By employing the inwards current as the indicator, fumarate injection resulted in uniform current peak which showed high specificity. A linear calibration curve with high regression factor ($R^2=0.9997$) was obtained with extremely wide fumarate concenrations (2 μM to 10 mM). The biosensing method developed showed good reliability, and had lower LOD than reported physical–chemical or biosensing methods. Trace monitoring may be further developed by integrating chip design or microfluid devices, and cell immobilization or special device design for practical application is also worth to be explored. To the best of our knowledge, this is the first biosensing system based on bacterial inwards electron transfer flow, and also is the first electrochemical method for fumarate detection. The idea to employ the bacterial inherent electron transfer pathway and redox enzyme for constructing bioelectrochemical sensing system, adds new dimension to whole-cell biosensor design.

Acknowledgements

The authors sincerely acknowledge the financial supports from Specialized Research Fund for the Doctoral Program of Higher Education (Ministry of Education, 20133227120014), Natural Science Foundation of Jiangsu Province (BK20130492), 'Six Talent Peaks' program (2012-NY-029, Jiangsu Province, China), and a project funded by the Priority Program Development of Jiangsu Higher Education Institutions (China).

Appendix A. Supplementary material

Supplementary data associated with this article can be found in the online version at http://dx.doi.org/10.1016/j.bios.2014.12.035.

References

Abboud, R., Popa, R., Souza-Egipsy, V., Giometti, C.S., Tollaksen, S., Mosher, J.J., Findlay, R.H., Nealson, K.H., 2005. Appl. Environ. Microb. 71, 811–816.
Baati, T., Horcajada, P., Gref, R., Couvreur, P., Serre, C., 2011. J. Pharmaceut. Biomed. 56, 758–762.
Barden, T.J., Croft, M.Y., Murby, E.J., Wells, R.J., 1997. J. Chromatogr. A 785, 251–261.
Blatny, P., Kvasnicka, F., Kenndler, E., 1996. J. Chromatogr. A 737, 255–262.
D'Souza, S.F., 2001. Biosens. Bioelectron. 16, 337–353.
Ganesh, I., Ravikumar, S., Lee, S.H., Park, S.J., Hong, S.H., 2013. J. Biotechnol. 168, 560–566.
Golitsch, F., Bucking, C., Gescher, J., 2013. Biosens. Bioelectron. 47, 285–291.
Jham, G.N., Fernandes, S.A., Garcia, C.F., da Silva, A.A., 2002. Phytochem. Anal. 13, 99–104.
Kim, B.H., Chang, I.S., Gil, G.C., Park, H.S., Kim, H.J., 2003. Biotechnol. Lett. 25, 541–545.
King, A., Selak, M.A., Gottlieb, E., 2006. Oncogene 25, 4675–4682.
Kvasnicka, F., Voldrich, M., 2000. J. Chromatogr. A 891, 175–181.
Lee, H.S., Wrolstad, R.E., 1988. J. Assoc. Off. Anal. Chem. 71, 789–794.
Leys, D., Tsapin, A.S., Nealson, K.H., Meyer, T.E., Cusanovich, M.A., Van Beeumen, J.J., 1999. Nat. Struct. Biol. 6, 1113–1117.
Li, D.B., Cheng, Y.Y., Wu, C., Li, W.W., Li, N., Yang, Z.C., Tong, Z.H., Yu, H.Q., 2014a. Sci. Rep. 4, 3735.
Peng, L., You, S.J., Wang, J.Y., 2010. Biosens. Bioelectron. 25, 2530–2533.
Pollard, P.J., et al., 2005. Hum. Mol. Genet. 14, 2231–2239.
Ross, D.E., Flynn, J.M., Baron, D.B., Gralnick, J.A., Bond, D.R., 2011. PLOS One 6, e16649.
Ryu, H.W., Kang, K.H., Yun, J.S., 1999. Appl. Biochem. Biotechnol. 77-79, 511–520.
Schenkmayerova, A., Bucko, M., Gemeiner, P., Katrlik, J., 2013. Biosens. Bioelectron. 50, 235–238.
Siegel, R., Naishadham, D., Jemal, A., 2012. CA-Cancer J. Clin. 62, 10–29.
Sokullu, E., Palabiyik, I.M., Onur, F., Boyaci, I.H., 2010. Eng. Life Sci. 10, 297–303.
Su, L.A., Jia, W.Z., Hou, C.J., Lei, Y., 2011. Biosens. Bioelectron. 26, 1788–1799.
Tang, X.J., Zhang, T.T., Liang, B., Han, D.F., Zeng, L.X., Zheng, C., Li, T., Wei, M.D., Liu, A. H., 2014. Biosens. Bioelectron. 60, 137–142.
Thomas, A.W., Garner, L.E., Nevin, K.P., Woodard, T.L., Franks, A.E., Lovley, D.R., Sumner, J.J., Sund, C.J., Bazan, G.C., 2013. Energy Environ. Sci. 6, 1761–1765.
Tomlinson, I.P.M., et al., 2002. Nat. Genet. 30, 406–410.
Toro, J.R., Nickerson, M.L., Wei, M.H., Warren, M.B., Glenn, G.M., Turner, M.L., Stewart, L., Duray, P., Tourre, O., Sharma, N., Choyke, P., Stratton, P., Merino, M., Walther, M.M., Linehan, W.M., Schmidt, L.S., Zbar, B., 2003. Am. J. Hum. Genet. 73, 95–106.
Trifiro, A., Saccani, G., Gherardi, S., Vincini, E., Spotti, E., Previdi, M.P., Ndagijimana, M., Cavalli, S., Reschiotto, C., 1997. J. Chromatogr. A 770, 243–252.
Wakayama, M., Aoki, N., Sasaki, H., Ohsugi, R., 2010. Anal. Chem. 82, 9967–9976.
Wang, X., Gao, N.S.J., Zhou, Q.X., 2013. Biosens. Bioelectron. 43, 264–267.
Webster, D.P., TerAvest, M.A., Doud, D.F.R., Chakravorty, A., Holmes, E.C., Radens, C. M., Sureka, S., Gralnick, J.A., Angenent, L.T., 2014. Biosens. Bioelectron. 62, 320–324.
Wu, R., Cui, L., Chen, L., Wang, C., Cao, C., Sheng, G., Yu, H., Zhao, F., 2013. Sci. Rep. 3, 3307.

Yang, M., Soga, T., Pollard, P.J., Adam, J., 2012. Front. Oncol. 2, 85.
Yang, M., Soga, T., Pollard, P.J., 2013. J. Clin. Investig. 123, 3652–3658.
Yong, Y.C., Zhong, J.J., 2009. Biosens. Bioelectron. 25, 41–47.
Yong, Y.C., Yu, Y.Y., Zhang, X., Song, H., 2014. Angew. Chem. Int. Ed. 53, 4480–4483.
Yu, Y.Y., Chen, H.L., Yong, Y.C., Kim, D.H., Song, H., 2011. Chem. Commun. 47, 12825–12827.